Optimization of the Reconfiguration Planning of Cyber-Physical Production Systems with Delta-Like Architecture*

Jan Brinker, Dominic Ring, Marco Lübbecke, Yukio Takeda, and Burkhard Corves

Abstract— **Data availability and modular design of modern production systems allow companies to respond flexibly to changing market conditions and process requirements. Against this background, this contribution presents tools to automatically identify energy efficient (re)configuration patterns. Therefore, market studies are used to reveal industrially relevant demand-related handling tasks and potential configurations for the well-known Delta parallel robot, as well as recent design modifications extending its field of application. In this context, optimization approaches are innovatively employed to effectively reduce the configuration space by discarding infeasible candidates and eventually solve the problem of simultaneous selection and allocation of configurations, such that a set of given handling tasks is performed in the most energy efficient way. Additionally, kinematic constraints are included in order to maintain the throughput rates of the underlying system. The approach is easily transferable to a system layout with reconfigurable, but also predetermined subsystems.**

I. Introduction

Modern industries are characterized by the tension between global competitive pressure and intensive price war. At the same time, customers demand a greater variety of products with specifications changed in ever-shorter intervals. In the course of the fourth industrial revolution it can be observed that (1) the demand for industrial automation continues to increase steadily, (2) production systems are characterized by intelligent acquisition of information and targeted use of smart data, and (3) economically friendly value added and green manufacturing have become important selling points of modern industries. Thus, there is a growing demand for efficient and sustainable robotic systems. Generally, the fourth industrial revolution or Industry 4.0 is associated with two aspects. On the one hand, "Cyber-Physical Systems" (CPS) denote real physical systems and products, which are able to communicate with a data infrastructure. On the other hand, the "Internet of Things" (IoT) enables the digital integration of production and cooperative networks of companies and employees as well as machines and products. It is obvious, that CPS and IoT create new opportunities for production planning. An economical production of lot size 1 however, requires both flexibility as well as efficiency. Measures tackling this dichotomy have grown in scope and importance over the last years.

*This work is supported by the German Academic Exchange Service (DAAD) with funds from the Federal Foreign Office (FFO).

Jan Brinker, Dominic Ring, and Burkhard Corves are with the Institute of Mechanism Theory, Machine Dynamics and Robotics, RWTH Aachen University, Aachen, Germany; e-mail: brinker@igmr.rwth-aachen.de.

Marco Lübbecke is with the Chair of Operations Research, RWTH Aachen University, Aachen, Germany; e-mail: luebbecke@or.rwth-aachen.de.

Yukio Takeda is with the Department of Mechanical Engineering, Tokyo Institute of Technology, Tokyo, Japan; e mail: takeda@mech.titech.ac.jp.

As a result, production systems are no longer tailored to single products and requirements but deal with a large number of highly diverse products. In this context, reconfigurability empowers companies to meet changing requirements on a single production system. While modern production systems are already designed in modular ways, allowing for flexibly responding to changing requirements by changing or adding modules, key aspects of future strategies still focus on flexibility and agility [1]. Given the indicated reconfigurability of systems, essential success factors of future production systems are tools to (automatically) identify suitable (re)configuration patterns of the system in order to fulfill the requirements determined by current process specifications.

Against this background, this contribution is concerned with the following scenario. Imagine an assembly line with handling objects of great diversity (e.g., variable size or weight) resulting from highly fluctuating known order streams. These objects may impose different requirements (e.g., payload, workspace, or degrees-of-freedom (dof) requirements) on the limited number of handling systems available. The number of available systems is restricted to p due to limited factory areas and fixed costs. Then using p identical handling systems each serving all handling tasks may be less efficient than using the same number of systems with optimized configurations. The set of p handling systems with known information about the forthcoming product stream and its requirements can be referred to as cyber-physical production system. Then, the challenging problem is to optimally select a fixed number of configurations from a given configuration space and simultaneously allocate them to a set of handling tasks in the most energy efficient way.

The following study is based on the widespread Delta parallel robot and recent design modifications extending the translational fully parallel architecture to serial-parallel designs with up to three additional rotational dof. Focusing on functional and dimensional reconfiguration possibilities, it is demonstrated that the underlying system is well suited for applications in the field of reconfiguration planning. Therefore, Delta-specific reconfiguration possibilities are introduced in Sect. II. Based on that, the optimization approach is presented in Sect. III. As input data, demand-related handling tasks and potential configurations are derived. The average energy consumption and the input transmission characteristics serve as target value and kinematic constraint, respectively (Sect. IV). In this context, an efficient dynamic modeling approach for the extended Delta robots is presented. The optimization problem is then solved by applying sophisticated operations research techniques. The related analysis and its results are presented in Sect. V.

978-1-5386-6380-6/18/$31.00 ©2018 IEEE

II. RECONFIGURABLE DELTA-LIKE ROBOTS

The niche market of parallel robots is dominated by 6-dof Gough/Stewart platforms [2], [3] for highly dynamic flight or driving simulation and 4-dof Delta parallel robots [4] for high-speed pick-and-place applications with light-weight objects. The original 4-dof Delta robot design is composed of a fully parallel architecture with three identical kinematic chains of the type 3-R(SS)$_2$ and one additional telescopic chain of the type RUPUR. In consequence, the three proximal links of the parallel architecture are rotationally actuated and connected with the platform by three spatial parallelograms (here denoted as distal links, Fig. 1). With this design, the platform exhibits three translational dof and one additional rotational dof. The ABB IRB 360 Flexpicker is probably the best-known industrial variant of this type. The expiration of Clavel's patents in December 2006 (Europe) and December 2007 (USA) paved the way for market entries of many new manufacturers. Today, more than 10 years later, increasing competition has led to many different design modifications. Therefore, by adding a fourth kinematic chain to the parallel architecture a Schoenflies motion can be realized too. Such concepts however require articulated moving platforms with internal mobility (e.g., Adept Quattro) or careful arrangement of the four kinematic chains among each other in order to allow for rigid moving platforms (e.g., the 4-dof version of the Blue Workforce Ragnar).

Extending the field of application to handling tasks with up to six dof (e.g., assorting, tooling, or measuring tasks) and/or with heavy-weight objects (e.g., stacking or packing tasks), alternative design modifications follow the original concept and add up to three additional serial chains to different attachment points within the basic parallel design.

A general definition describes reconfiguration as the process of repeatedly changing and rearranging the components of a system in a cost-effective way [5]. In regards to parallel robots, reconfiguration is used in many fields and contexts, e.g, [6]–[12]. Here, the reconfiguration of Delta parallel robots is distinguished between dimensional reconfiguration (corresponding to the notion of variable-dimension modules or geometry morphing) and functional reconfiguration (by adding or removing additional serial chains to the classical parallel Delta architecture).

A. Dimensional Reconfiguration

The Delta parallel robot offers many possibilities for dimensional reconfiguration. Based on this, basic variable dimensions for each kinematic chain are given by

- the relative position of the actuated revolute joint to the origin of the frame (three dimensions $\boldsymbol{r}_{F,i}$),
- the orientation of the actuated revolute joints or actuation axes, respectively, about the horizontal axis X_i and/or to the vertical axis Z_i of the local chain-based coordinate system (two dimensions δ_i and γ_i),
- the length of the proximal link (one dimension $l_{PL,i}$),
- the length of the distal link (one dimension $l_{DL,i}$), and
- the relative position of the midpoint of the pair of passive spherical joints to the origin of the platform (three dimensions $\boldsymbol{r}_{P,i}$).

There are only a few contributions in literature regarding dimensional reconfiguration of Delta parallel robots. Miller [13] analyzes the influences of changing the actuation axes on the workspace shape and size. Interestingly, the recent industrial variant Ragnar robot with four kinematic chains by the Danish company Blue Workforce adapts the concept of tilted motor axes. Dynamic reconfiguration concepts of the motor positions, given by $\boldsymbol{r}_{F,i}$, and lengths of the proximal and distal links ($l_{PL,i}$ and $l_{DL,i}$) are proposed and analyzed in [14].

In recent studies, linear actuation is added to the original system in order to dynamically vary the frame radius $\boldsymbol{r}_{F,i}$ while simultaneously adapting the relative height of the actuators to the frame [15]. Pfurner [16] replaces the rigid platform by Bricard's orthogonal 6R-linkage, an actuated closed overconstrained chain allowing for a variable platform geometry with $\boldsymbol{r}_{P,i}$.

Interestingly, the inventor Clavel [4] already mentioned in his dissertation in 1991 that the Delta robot is distinguished by its modularity and the fact that some components are found in several identical copies in one robot. Therefore, presuming a symmetric design and reconfiguration (i.e., symmetric circular arrangement of the frame- and platform-related joints as well as identical kinematic chains), a Delta robot contains three identical modules for the proximal links and six identical modules for the connecting rods of the distal links. Other dimensions, such as link radii and wall thicknesses are imaginable for reconfiguration but not considered in this study.

B. Functional Reconfiguration

The Delta robot is considered functionally reconfigurable by attaching additional chains to the parallel architecture in order to add rotational dof to the overall system. Analyses of the portfolio of Delta manufacturers [17] show that the majority of commercial variants are 4-dof variants with a telescopic shaft driven from the frame, e.g., the ABB IRB 360 Flexpicker or the Adept Hornet 565. In other variants, a 2- or 3-dof rotational head or serial robotic wrist (type RR or RRR, respectively) is attached to the platform and driven by two or three additional motors, hereafter referred to as wrist motors. Based on the architecture of the translational parallel robot, four different functional extensions E can be identified and classified based on the attachment points of the wrist motors. Therefore, the wrist motors can be attached to

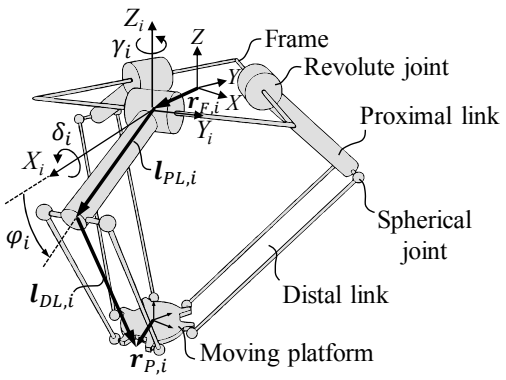

Figure 1. Geometric relations and notations of the 3-dof Delta robot

- the frame (E_F),
- the proximal links (E_{PL}),
- the distal links (E_{DL}), or
- the platform (E_P).

Functional extensions to the frame (E_F), driving a 2-dof serial wrist (resulting in 5-dof), are for example offered by Codian, employing two separate telescopic chains, or by MAJAtronic, employing two coaxially guided telescopic chains. The latter results in a rather bulky design. Both designs are considered extendable to 6-dof applications. FANUC holds a patent for a 6-dof version with particular universal joints, allowing for linear motion. Due to design reasons, attachments of the wrist motors to the proximal links (E_{PL}) cannot be observed in industrial variants. However, placing the wrist motors into the parallelograms of the distal links (E_{DL}) circumvents the telescopic design while offering similar dynamic characteristics compared to E_F [18]. Such variants are patented by FANUC and offered as 4-dof as well as 6-dof variants. Direct drives at the platform (E_P) are commonly offered as 4-dof versions for the handling of light-weight objects, allowing for small motor sizes. Fig. 2 illustrates 6-dof variants with functional extensions including industrial application examples and graph representations.

III. Modeling Approach

A cyber-physical production system (CPPS) may be highly flexible in the sense that its configurations can be adapted (i.e., the system can be reconfigured) in accordance with forthcoming product streams and known requirements. The CPPS is represented by a set of p configurations from a set of reconfigurable handling systems (given here by all possible configurations of Delta parallel robots with functional extensions) and is used to handle a set of known objects. The challenge now lies in simultaneously selecting p configurations of the set and assigning tasks to the selected ones, such that the overall efficiency is maximized. This resembles a standard problem in operations research known as location problem.

Previous work in [6] presents a novel and rigorous approach that effectively formulates and solves the problem as a standard binary integer p-median problem. The applicability of the original model however is limited due to high memory usage in case of large data sets. Nonetheless, general feasibility was proven for a rather small test instance of 200 handling tasks and 2,250 reconfiguration possibilities. In this contribution,

- in order to reduce high memory of the original model, an alternative solution technique known as column generation is presented,
- in order to obtain a minimal configuration space, feasible ranges for the dimensional reconfiguration are determined without discarding viable configurations based on poor user experience, and
- in order to ensure high throughput rates of the system, a minimum requirement is imposed for the input transmission characteristics of the reconfigurable Delta robots.

3-$\underline{R}(SS)_2$:

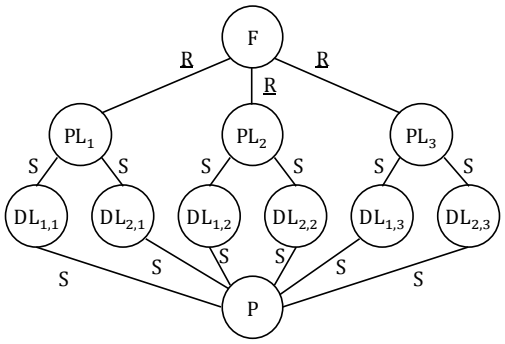

$E_{F,i}$: $\underline{R}$UPU (e.g., Codian D5, MAJAtronic RL5-750)

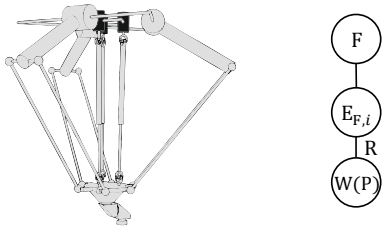

$E_{PL,i}$: U$\underline{R}$PU (not applicable, theoretical example)

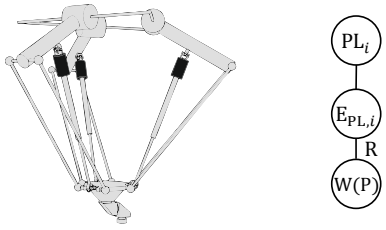

$E_{DL,i}$: R$\underline{R}$U (e.g., FANUC M-2iA, FANUC M-3iA)

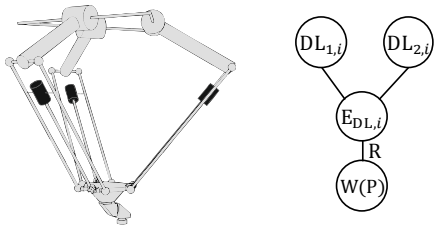

$E_{P,i}$: $\underline{R}$ (e.g., Kawasaki YF03N, Yaskawa MPP3S)

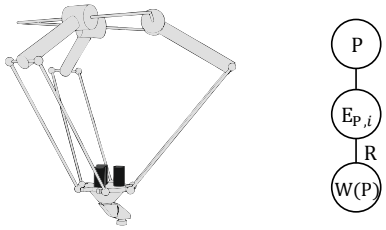

Figure 2. Graph representations of the 3-$R(SS)_2$ variant and functional extensions

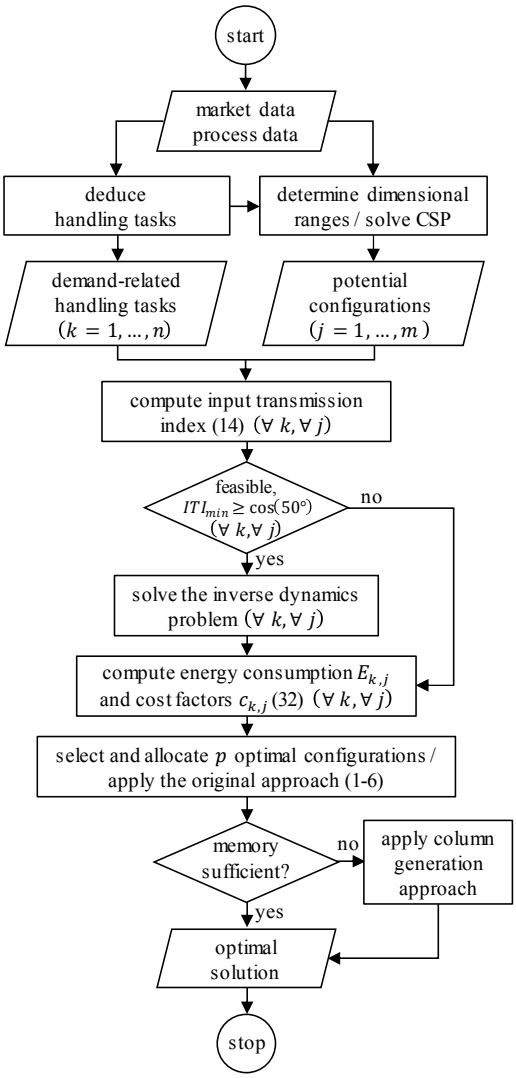

Figure 3. Modeling approach

The original model and the column generation approach are introduced in Sections IV.A and IV.B. The input data are defined by the task space (set of handling tasks) and the configuration space (set of potential configurations). Market figures are used to generate the task space (Sect. IV.C), whereas fixed value discretization is used to generate the set of potential dimensional reconfigurations. The configuration space is then composed of the combination of all dimensional and functional reconfiguration possibilities (Sect. IV.D). The energy consumption serves as an indicator to assess the allocations of tasks to configurations (Sect. IV.E). Fig. 3 depicts the overall modeling approach.

IV. Model Formulation

Generally speaking, a p-median problem is a location problem, in which the number of medians to be located is given. In the simple case, the objective then is to minimize the sum of median-demand distances weighted with the respective demand volume [19]. In this case, the median and demand locations are given as configurations and handling tasks, respectively. Other practical examples can be found for example in [20]–[25].

A. Original Approach

The standard p-median problem is formulated as [6]:

$$\Phi = \min \sum_{k \in A} \sum_{j \in M} c_{k,j} y_{k,j} \tag{1}$$

such that

$$\sum_{j \in M} y_{k,j} = 1 \qquad \forall\, k \in A \tag{2}$$

$$\sum_{j \in M} x_j = p \tag{3}$$

$$y_{k,j} \leq x_j \qquad \forall\, k \in A, \forall\, j \in M \tag{4}$$

$$x_j \in \{0, 1\} \qquad \forall\, j \in M \tag{5}$$

$$y_{k,j} \in \{0, 1\} \qquad \forall\, k \in A, \forall\, j \in M \tag{6}$$

where

- A is the set of handling tasks (with $k = 1, \dots, n$),
- M is the set of potential configurations (with $j = 1, \dots, m$), and
- $c_{k,j}$ is the costs of configuration j performing task k.

The binary decision variables are denoted as

- $x_j = 1$, if configuration j applies (0 otherwise) and
- $y_{k,j} = 1$, if a task k is allocated to a configuration j (0 otherwise).

With constraint (2) it is ensured that each task k is allocated to only one configuration j. Constraint (3) sets the number of configurations to be selected to p. Finally, constraint (4) ensures that a task k can only be allocated to a configuration j if j is part of the selected configurations. A penalty applies for $c_{k,j}$ if configuration j cannot perform task k. Note that model (1-6) is able to optimally select and simultaneously optimally assign tasks from the entire configuration space.

B. Column Generation Approach

The p-median problem is known to be NP-hard. Thus, computational costs to solve it increase exponentially with the problem size [26]. In order to reduce the computational costs, column generation represents an alternative solution technique, which does not require full enumeration of all possibilities [27]. The most famous application example of column generation is the cutting stock problem for a given demand. In this case, the objective is to minimize the number of used logs. However, instead of analyzing all potential cutting patterns, the patterns are generated within the optimization itself [28]. Against this background, Lorena and Senne [29] propose a column generation approach for solving a capacitated p-median problem. Following their approach, the original model (1-6) is reformulated as set partitioning problem and relaxed with regard to the binary decision variables. Presuming the resulting master problem to be too hard to solve, only a subset of all reconfiguration possibilities is taken into account. This

subset S is then solved as a so-called restricted master problem (RMP), i.e.,

$$\Phi_{RMP} = \min \sum_{s \in S} c_s x_s \tag{7}$$

such that

$$\sum_{s \in S} \lambda_{k,s} x_s \geq 1 \qquad \forall\, k \in A \tag{8}$$

$$\sum_{s \in S} x_s = p \tag{9}$$

$$x_s \in [0,1] \qquad \forall\, s \in S \tag{10}$$

with the column cost c_s, the relaxed decision variable x_s, and the scalar value $\lambda_{k,s}$ of the $(n \times m)$-matrix Λ, storing the current configuration states $\lambda_{k,j}$, where $\lambda_{k,j} = 1$, if a configuration j can perform task k and $\lambda_{k,j} = 0$ otherwise.

The RMP constitutes a so-called set covering problem. It consists of s different subsets, where each subset is represented as one unique configuration. The decision variable x_s is equal to 1, if subset s is part of the solution. Solving the RMP yields a dual solution vector $(\pi_k \quad \mu)^T$. It contains a value π_k for each task k and a value μ denoting the cost for employing an additional configuration. Being a comparison vector, which accounts for the improvement, it is used to generate new columns. Therefore, to obtain potential new columns, m individual knapsack problems need to be solved, i.e.,

$$v(knap^{\pi})_j = \min \sum_{k \in A} (c_{k,j} - \pi_k) x_{k,j} \tag{11}$$

such that

$$x_{k,j} \in \{0,1\} \qquad \forall\, k \in A, \forall\, j \in M \tag{12}$$

The m individual knapsack problems each contain separate objective values, cf. (11). If an objective value of the knapsack is smaller than μ, the corresponding column is added to the RMP. The original cost of allocating task k to configuration j is then compared to the dual solution vector. If the comparison results in a negative value, the decision variable $x_{k,j}$ is set to 1. The RMP is then solved with the columns newly added to S. The process is repeated until no new columns are found. Since the solution to the RMP may not be integral, a standard branch-and-bound procedure needs to be applied subsequently. Note that, since capacity and occupancy figures are neglected, there is no capacity limit on the configurations, which also applies to the knapsack problems in this study. Infeasible allocations are already accounted for by penalties for $c_{k,j}$, cf. Sect. IV.A.

C. Task Space

Market analyses of commercially available Delta robot variants based on [17] reveal the distributions of payload, workspace (WS) diameter, and dof as shown in Tab. I. The resulting data would need to be adjusted by using currently unavailable process figures and actual product streams. In real application however, data can be extracted from current demand numbers or demand statistics (cf. previous study [22]).

TABLE I. SHARES OF WORKSPACE DIAMETER, PAYLOAD, AND DOF

WS	WS-∅ D_1 [m]	Share [%]	Payload [kg]	Share [%]	dof [–]	Share [%]
A	≤ 0.8	28	0.1–3	62	3	33
B	0.8–1.2	40	3–6	18	4	52
C	1.2–1.6	31	6–9	4	5	7
D	1.6–2	1	9–12	4	6	8
			12–20	12		

The workspaces may consist of a cylinder and a conical portion adjacent to it. For the conical portion, the diameter is set to $D_2 = 0.75 \cdot D_1$, where D_1 denotes the diameter of the cylinder. The overall heights of the workspaces A and B as well as C and D are respectively set to 0.30 m and 0.50 m. The heights of the cylinder and the cone Z_1 and Z_2 account for respectively 3/5 and 2/5 of the respective overall height. The center of the connecting surface between cylinder and cone determines the relative position $\boldsymbol{P_0} = [0, 0, Z_{0,k,j}]$ of the workspace to the origin of frame O, where $Z_{0,k,j}$ is identified by preceding kinematic optimizations for each combination of task k and configuration j. Therefore, $Z_{0,k,j}$ is determined such that the motion transmission from the input to the output is maximal over the respective workspace. The related input transmission characteristics are commonly assessed by taking into account the angle between the velocity $\boldsymbol{v}_{k,j,i}$ at the tip of the proximal link and the direction of the force transmitted to the output link along the distal link. This angle is known as the pressure angle $\eta_{k,j,i}$ of the input transmission [30]. Its cosine value is

$$\rho_{k,j,i} = \cos(\eta_{k,j,i}) = \hat{\boldsymbol{v}}_{k,j,i}^T \, \hat{\boldsymbol{l}}_{DL,k,j,i} \tag{13}$$

with the circumflex denoting a normalized vector. The best transmission thus occurs when the directions of velocity and force coincide. Consequently, the minimum of the absolute pressure angles' cosine among all three kinematic chains over the entire workspace (WS), given by

$$ITI_{k,j} = \min_{\mathrm{WS}_k} \left(\min \left(\left| \rho_{k,j,i} \right| \right) \right) \quad \forall\, i = \{1,2,3\} \tag{14}$$

should be maximized.

In order to assess the energy consumption of a configuration j performing a task k, industrially-relevant trajectories are defined similar to [31]. The underlying paths are randomly rotated about the vertical axis in steps of $\pi/6$ for higher variance of the indicators. Finally, $n = 5{,}150$ tasks are generated to form set A. It is ensured that all combinations of workspace sizes and dof occur at least once in A. Otherwise, it is possible that for a randomly generated task set, WS D with a share of only 1 % does not occur in combination with all dof requirements.

D. Configuration Space

In order to achieve the highest possible efficiency, a planner may be interested in determining the greatest possible configuration space. However, in order to ensure reasonable computation times or even solvability of the optimization approaches, the configuration space should be the smallest

possible. In addition to the given requirements stemming from the task space definition (which in turn are specified process requirements and the related requests of the customer), other requirements may be based on

- practical implementation (e.g., restrictions of the motion angle of spherical joints, the distance between neighboring spherical joints of two distinct kinematic chains, or the actuation joint range),
- kinematic characteristics (e.g., dead center positions at critical corner points of the prescribed workspace),
- performance criteria (e.g., minimum input transmission characteristics, corresponding to allowable pressure angles, or a minimum ratio of workspace to installation space), or
- experience.

Applying requirements based on experience may lead to unneeded and undesired reductions of the configuration space (by potentially discarding valid configurations). Using solely mandatory requirements, a set of parametric relations or constraints can be derived in order to reduce the feasible parameter ranges for dimensional reconfiguration. Serving as an example, the maximum pressure angle provides a lower bound for Z_0 in the X_iZ_i-plane, i.e.,

$$r_i = \sqrt{l_{PL}^2 + l_{DL}^2 - 2l_{PL}l_{DL}\cos(\pi/2 + \eta_i)} \geq Z_0 + Z_2 \quad (15)$$

where r_i can be described as maximum reach of a kinematic chain without exceeding the allowable pressure angle, which is usually limited to $\eta_i \leq 50°$ [32]. A total number of eleven constraints are used to reduce the design parameter ranges. For the sake of brevity, their derivation is not shown here. The determination of feasible dimensional ranges constitutes a constraint satisfaction problem (CSP). In general, a CSP consists of a set of variables, a set of domains (representing the dimensional ranges), and a set of constraints. CSP are NP-complete, which means they can be optimally solved in polynomial time using non-deterministic methods. The optimal solution then provides exact intervals or ranges for the parameters or reconfigurable dimensions, respectively, for which all constraints are satisfied. In other words, each dimension is minimized and maximized while satisfying all constraints. The related CSP is implemented and solved in Advanced Interactive Multidimensional Modeling System (AIMMS) using the commercial constraint programming engine IBM® ILOG® CPLEX® CP Optimizer [33][34]. Note that random sampling methods or gradient-based optimization methods may be used as simple alternatives, but do not provide exact bounds since particular outliers remain undetected.

Based on Sect. II, the set M of potential configurations is generated combining discrete values for selected dimensions within the optimized ranges, functional extensions, and number of dof. For practical and symmetrical reasons, the orientations of the motor axes are set to zero, the platform radius is fixed to $r_P = 0.07$ m, and the theoretical and inefficient functional extensions E_{PL} and E_P are discarded. The boundaries of the dimensions for discretization are set, taking into account the minimum and maximum domains as resulting from solving the CSP for the four workspaces.

TABLE II. DIMENSIONAL AND FUNCTIONAL CONFIGURATIONS

	r_F [m]	l_{PL} [m]	l_{DL} [m]	Ext. [–]	dof [–]
	0.200	0.200	0.600	E_F	3
	0.250	0.250	0.650	E_{DL}	4
	0.300	…	…	NONE	5
		0.800	1.800		6
$n_{S,P}$	3	13	24	3	4

Discretization of the dimensions with step sizes according to Table II and combination of all potential candidates leads to $\prod n_{S,P} = 3 \cdot 13 \cdot 24 \cdot 3 \cdot 4 = 11{,}232$ configurations, where $n_{S,P}$ denotes the number of configurations of the reconfiguration possibility. Note that $l_{DL} = 0.85$ m is out of all ranges leading to 24 instead of 25 dimensions for l_{DL}. Candidates without extensions but more than three dof and, vice versa, candidates with extension but less than four dof must be discarded. This finally results in $m = 3 \cdot 13 \cdot 24 \cdot \left(|\{E_F, E_{DL}\}| \cdot |\{4,5,6\}| + |\{NONE\}| \cdot |\{3\}|\right) = 6{,}552$ potential configurations. Note that even the maximum values for the lengths of the distal links are conceivable in industrial applications (see for instance MAJAtronic/Autonox 24 RL3-2000 with l_{DL} = 1.650 m).

E. Performance Measure (Objective)

The average energy consumption serves as target value for the optimization. Thus, the actuation speeds and torques are required for the derivation of the objective value. While the actuation speeds can be easily obtained from mapping the platform velocity $\boldsymbol{v}_P$ to the actuation velocities $\dot{\boldsymbol{\varphi}}$ by the manipulator Jacobian matrix $\boldsymbol{J}_M$, i.e.,

$$\boldsymbol{v}_P = \boldsymbol{J}_M \dot{\boldsymbol{\varphi}} \quad (16)$$

sophisticated modeling techniques are required to obtain the required driving torques of the functionally extended Delta parallel robots performing a given trajectory. This is emphasized taking into account that, in order to optimize (1) or (7), $n \cdot m = 33{,}742{,}800$ cost values $c_{k,j}$ need to be computed. Detailed derivations of the fundamental kinematic and dynamic relations of functionally extended Delta robots are presented in a previous study [18].

The most common analytical approaches for dynamic modeling of parallel robots are the Newton-Euler Formulation, the Lagrangian Formulation, and the Lagrange-d'Alembert Principle of Virtual Work [34]. Alternatively, projection methods such as Kane's equations [35] or the Method of the Natural Orthogonal Complement (NOC) [36] efficiently circumvent the non-working constraint forces of the Newton-Euler formulation, the cumbersome derivation of the link Jacobian matrices following the virtual work principle, and expensive time differentiation of the Lagrangian. The simple idea of Kane's formulation is to dot-multiply Newton's second law by a proper vector and herewith project the resultants of the applied and inertia wrenches along the related vectors of partial velocities. Recalling the principle of virtual work due to the applied and inertia forces $\boldsymbol{f}_b$ and $\boldsymbol{f}_b^*$ in the COG of a body b, it follows with the virtual displacement $\boldsymbol{\chi}_b$

$$\delta W = \delta \boldsymbol{\chi}_b (\boldsymbol{f}_b + \boldsymbol{f}_b^* + \boldsymbol{f}_b^C) = \delta \boldsymbol{\chi}_b (\boldsymbol{f}_b + \boldsymbol{f}_b^*) = 0 \quad (17)$$

where the virtual work of the constraint forces $\boldsymbol{f}_b^C$ vanishes. Then, without loss of generality, the virtual displacement can be written as

$$\delta \boldsymbol{\chi}_b = \frac{\partial \boldsymbol{\chi}_b}{\partial q_i} \delta q_i \quad (18)$$

with q_i as generalized coordinates. Time-differentiation of $\boldsymbol{\chi}_b$ leads to

$$\dot{\boldsymbol{\chi}}_b = \frac{\partial \boldsymbol{\chi}_b}{\partial q_i}\frac{dq_i}{dt} + \frac{\partial \boldsymbol{\chi}_b}{\partial t} = \frac{\partial \boldsymbol{\chi}_b}{\partial q_i}\dot{q}_i + \frac{\partial \boldsymbol{\chi}_b}{\partial t} \quad (19)$$

where the last part is zero for the given scleronomous constraints. The generalized speeds are denoted by $\dot{q}_i$. Now, for the partial differentiation of $\dot{\boldsymbol{\chi}}_b$ with respect to $\dot{q}_i$, it can be stated

$$\frac{\partial \dot{\boldsymbol{\chi}}_b}{\partial \dot{q}_i} = \frac{\partial \boldsymbol{\chi}_b}{\partial q_i} \quad (20)$$

With (18) and (20) it eventually follows

$$\delta \boldsymbol{\chi}_b = \frac{\partial \dot{\boldsymbol{\chi}}_b}{\partial \dot{q}_i} \delta q_i \quad (21)$$

Substituting (21) in (17) and cancellation of δq_i leads to [37]

$$\frac{\partial \dot{\boldsymbol{\chi}}_{b,i}}{\partial \dot{q}_i} (\boldsymbol{f}_b + \boldsymbol{f}_b^*) = 0 \quad (22)$$

Similarly, the relations for the moments and angular displacements can be derived. Finally, it follows the basic principle of Kane's equations that the sum of the applied and inertia forces ($\boldsymbol{F}_b$ and $\boldsymbol{F}_b^*$) and moments ($\boldsymbol{N}_b$ and $\boldsymbol{N}_b^*$) is projected in the directions of the partial derivatives of the linear and angular velocity vectors $\boldsymbol{v}_b$ and $\boldsymbol{\omega}_b$ according to the generalized speeds, i.e.,

$$W_i + W_i^* = \sum_{b=1}^{r} \frac{\partial \boldsymbol{v}_b}{\partial \dot{q}_i} (\boldsymbol{F}_b + \boldsymbol{F}_b^*) + \sum_{b=1}^{r} \frac{\partial \boldsymbol{\omega}_b}{\partial \dot{q}_i} (\boldsymbol{N}_b + \boldsymbol{N}_b^*) = 0 \quad (23)$$

for a system of $b = 1, \dots, r$ rigid bodies, where * denotes the inertia terms [35], [38]. Therefore, for each of the r rigid bodies of the (functionally extended) Delta robot, the sum of all generalized applied and inertia forces and moments ($\boldsymbol{W}$ and $\boldsymbol{W}^*$) is zero. For the three generalized coordinates φ_i of the basic 3-dof Delta robot, (23) can be expressed in a compact matrix form:

$$\boldsymbol{W} + \boldsymbol{W}^* = \boldsymbol{V} \cdot (\boldsymbol{F} + \boldsymbol{F}^*) + \boldsymbol{\Omega} \cdot (\boldsymbol{N} + \boldsymbol{N}^*) = \boldsymbol{0} \quad (24)$$

with $\boldsymbol{F}$ and $\boldsymbol{F}^*$ ($\boldsymbol{N}$ and $\boldsymbol{N}^*$) as $(3r \times 1)$-vectors containing the resultant applied and inertial forces (moments) for the rigid bodies $b = 1, \dots, r$ of the system and $\boldsymbol{V}$ and $\boldsymbol{\Omega}$ as $(3 \times 3r)$-matrices containing the partial derivatives of the linear and angular velocities $\tilde{\boldsymbol{v}}_{b,i}$ and $\tilde{\boldsymbol{\omega}}_{b,i}$, respectively, according to the generalized speeds, i.e.,

$$\tilde{\boldsymbol{v}}_{b,i} = \frac{\partial \boldsymbol{v}_b}{\partial \dot{q}_i} \quad (25)$$

and

$$\tilde{\boldsymbol{\omega}}_{b,i} = \frac{\partial \boldsymbol{\omega}_b}{\partial \dot{q}_i} \quad (26)$$

The actuation torques of the three main drives can then be extracted solving (24) for the applied moments $\boldsymbol{N}$, i.e.,

$$\boldsymbol{\tau} = \boldsymbol{\Omega} \cdot \boldsymbol{N} = -\boldsymbol{V} \cdot (\boldsymbol{F} + \boldsymbol{F}^*) - \boldsymbol{\Omega} \cdot \boldsymbol{N}^* \quad (27)$$

For the sake of brevity, the derivations of the partial velocities are not shown here.

The masses and mass moments of inertia of the bodies need to be adapted according to the dimensional reconfiguration possibilities. Therefore, the following assumptions apply (as introduced in [6]). The masses of the proximal and distal links are adapted by a linear scale factor

$$C_{i,j} = l_{i,j}/l_{i0} \quad (28)$$

i.e., the ratio of the length of link i in configuration j and the corresponding original value based on real robot data denoted by zero (as provided in [18]). As a simplification, the mass moment of inertia (about the perpendicular axes) I at the center of the proximal link is adapted by

$$C_{PL,i,j,I} = \left(l_{PL,i,j}/l_{PL,i0}\right)^2 \quad (29)$$

whereas for the connecting rods of the distal link (modeled as thin rods) the following applies

$$C_{DL,i,j,I} = \left(l_{DL,i,j}/l_{DL,i0}\right)^3 \quad (30)$$

Finally, the average energy consumption of a configuration j performing a task k can be derived by

$$E_{k,j} = \frac{1}{3}\sum_i \int_0^T \max\left(\tau_{k,j,i}\dot{\varphi}_{k,j,i}, 0\right) \cdot dt \quad (31)$$

where $\dot{\varphi}_{k,j,i}$ denotes the actuation velocity. Here, it is assumed that the braking energy cannot be recuperated. Therefore, $E_{k,j}$ serves as a performance indicator to assess the allocation of task k to configuration j. In order to guarantee superior motion transmission capabilities, in addition to the reachability of the prescribed workspace, a minimum input transmission index of $ITI_{k,j} \geq \cos(50°) \approx 0.642$, cf. (14), is ensured. Finally, the cost factor is given as

$$c_{k,j} = \begin{cases} E_{k,j}, & \text{feasible}, ITI_{min} \geq \cos(50°) \\ \infty, & \text{infeasible}, ITI_{min} < \cos(50°) \end{cases} \quad (32)$$

V. Analysis and Results

The kinematic and dynamic models were validated by experiments [18] and implemented in MATLAB®, in order to compute the $n \cdot m$ cost values $c_{k,j}$. The p-median problem was implemented using Python™ and then solved with Gurobi Optimizer [39]. Similarly, the column generation approach was implemented in MATLAB® and solved with Gurobi Optimizer. A production line is usually equipped with five to seven Delta robots. In this illustrative study, the production line is optimized using six configurations ($p = 6$). Accordingly, from 6,552 reconfiguration possibilities, six configurations are selected and optimally allocated to 5,150 known tasks.

TABLE III. OPTIMAL CONFIGURATIONS FOR $p = 6$

$p = 6$	Conf. 1	Conf. 2	Conf. 3	Conf. 4	Conf. 5	Conf. 6
r_F [m]	0.20	0.20	0.20	0.20	0.20	0.20
l_{PL} [m]	0.55	0.55	0.60	0.75	0.75	0.75
l_{DL} [m]	0.80	0.80	0.80	1.1	1.1	1.5
Ext. [–]	E_F	E_F	–	–	E_F	E_F
dof [–]	4	6	3	3	4	6
WS-Ø [m]	1.2	1.2	1.2	1.6	1.6	2.0
Cvg. [%]	34.3	10.6	22.1	10.2	16.3	6.5
$\overline{ITI_{min}}$	0.737	0.742	0.733	0.654	0.654	0.772

Tab. III summarizes the optimal solutions for a production line with a maximum of $p = 6$ configurations and minimal constraint for ITI. It can be seen that each configuration covers at least 6.5 % of all tasks and at maximum 34.3 %. Since energy consumption is used as target value, all extensions are related to the frame (i.e., E_F) in order to minimize the inertial effects of the additional bodies. In other words, E_F slightly dominates E_{DL} in respect of energy efficiency, which corresponds to the results of a previous comparative study in [18]. Tab. III also includes the mean input transmission index $\overline{ITI_{min}}$ of allocations to each configuration. Fig. 4 additionally summarizes the allocations of tasks to the configurations clustered according to the dof and workspace requirements. Note that the shares of dof and WS correspond to Tab. I. Configurations 1 to 3 exhibit similar dimensions and cover 3, 4, and 6 dof tasks as well as workspace sizes up to WS B. Configurations 4 and 5 have identical link lengths and thus, reach the same workspace WS C. However, only tasks with 3 and 4 dof are covered. In order to accomplish 6-dof tasks and/or the largest workspace WS D, it can be allocated to configuration 6. Interestingly, there is no configuration with 5 dof. Instead, all tasks with 5 dof are allocated to configurations 2 and 6 with 6 dof. Moreover, two allocation clusters are observed for the workspace requirements. Therefore, all tasks with workspaces WS A and WS B are accomplished by configurations 1 to 3, whereas tasks in WS C and WS D are allocated to configurations 4 to 6.

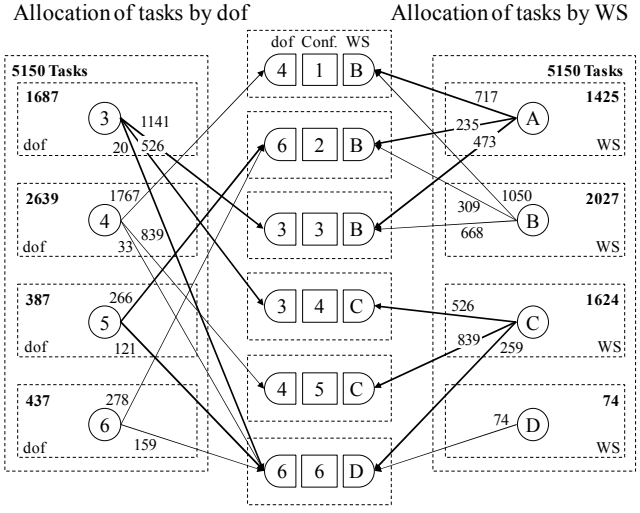

Figure 4. Allocation of tasks by dof and WS

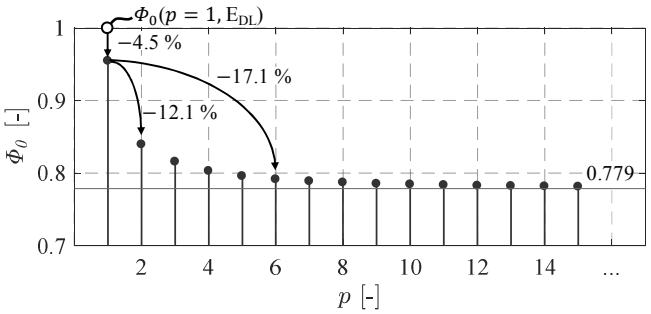

Figure 5. Normalized total energy consumption Φ_0 depending on the number of configurations p

Fig. 5 displays the normalized total energy consumption Φ_0 related to the number of configurations p, cf. (1). As normalization factor, the maximum energy consumption when allocating all tasks to the best configuration with functional extension(s) attached to the distal link(s) E_{DL} is taken into account, i.e., $\Phi_0(p = 1, E_{DL})$. Therewith, an energy saving of 4.5 % is achieved by applying the best dimensional variant with the functional configuration E_F covering all tasks instead of the most efficient variant of E_{DL}. Based on that, by applying two optimal configurations instead of only one, the total energy consumption drops by 12.1 %. The energy consumption degressively decreases reaching a threshold of 0.779 (corresponding to 18.4 % energy saving compared to the optimal solution for $p = 6$) for $p > 15$, which emphasizes the consistency of the approach. By allocating according to the optimal solution ($p = 6$), energy consumption is effectively reduced by 17.1 % compared to allocating all tasks to one configuration ($p = 1$). In this case, the optimal solution is given by configuration 6, which covers all tasks most efficiently.

The original binary integer programming problem was transformed to a relaxed problem and restricted to configuration subsets by applying a column generation approach. Then, by iteratively adding variables of the model, excessive memory usage of solving the original model formulation can be decreased at the cost of solving time. This proves to be beneficial when dealing with large problems and limited resources. Faster computational times of the column generation approach may for instance be achieved by further investigating for better starting solutions. Note that both approaches yield optimal solutions.

VI. CONCLUSION

This paper was concerned with optimization approaches for the reconfiguration planning of flexible cyber-physical production systems. Based on the analyses of functionally extended Delta parallel robots, it was shown that energy efficiency of a production line with multiple handling systems can be effectively reduced by adapting the system configurations to the known product stream and requirements. Due to this, operations research techniques were innovatively employed in order to optimally select a fixed number of configurations from the entire configuration space and simultaneously allocate the selected configurations to a set of handling tasks in the most energy efficient way. The performance of the optimization procedure was increased reducing the configuration space by analyzing parametric relations of the dimensional reconfiguration possibilities based

on practical implementation, kinematic characteristics, and performance criteria. The related constraint satisfaction problem was solved optimally without unneeded and undesired reductions of the configuration space (as commonly resulting from experience based requirements). Discretization of the dimensions can possibly be refined at the cost of already considerable computational times, though the practical benefit appears questionable. The proposed models are not only applicable to other reconfigurable production systems but also to factory layout planning with fixed system configurations. Final economical evaluation, however, requires the integration of set-up times and costs, initial procurement and operating costs, as well as capacity and occupancy figures.

REFERENCES

[1] Multi-Annual Roadmap (MAR) for Horizon 2020, SPARC Robotics, euRobotics AISBL, Brussels, 2017.

[2] V. E. Gough, "Contribution to discussion of papers on research in automobile stability, control and tyre performance," in *Proc. of the Inst. of Mechanical Engineers, Automobile Division*, 1956, pp. 392–394.

[3] D. Stewart, "A platform with six degrees of freedom," in *Proc. of the Institution of Mechanical Engineers*, vol. 180, no. 1, 1965, pp. 371–386.

[4] R. Clavel, "Conception d'un robot parallèle rapidé à 4 degrés de liberté," Ph. D. thesis, EPFL, Lausanne, 1991.

[5] R. M. Setchi and N. Lagos, "Reconfigurability and reconfigurable manufacturing systems state-of-the-art review," in *Proc. of the IEEE Int. Conf. on Industrial Informatics*, Berlin, June 2004.

[6] J. Brinker, M. E. Lübbecke, Y. Takeda, and B. Corves, "Optimization of the reconfiguration planning of handling systems based on parallel manipulators with Delta-like architecture", *IEEE Robotics and Automation Letters*, 2(3), 2017, additionally selected by CASE'17 Program Committee for presentation at the conference.

[7] A. Kumar Dash, I-M. Chen, S. H. Yeo, and G. Yang, "Task-oriented configuration design for reconfigurable parallel manipulator systems," *Int. J. of Computer Int. Manuf.*, vol. 18, no. 7, 2005, pp. 615–634.

[8] J. Schmitt, D. Inkermann, C. Stechert, A. Raatz, and T. Vietor, "Requirement oriented reconfiguration of parallel robotic systems," in *Robotic Sys. – App., Control and Programming*, 2012, pp. 387–410.

[9] T. Mannheim, M. Riedel, M. Hüsing, and B. Corves, "A New Way of Grasping PARAGRIP – The Fusion of Gripper and Robot," *Mechanisms and Machine Science: Grasping in Robotics*, vol. 10, 2012, pp. 433–464.

[10] F. Xi, Y. Li, and H. Wang, "A module-based method for design and analysis of reconfigurable parallel robots," in *Proc. of the IEEE ICMA*, Xi'an, August, 2010.

[11] A. Moosavian and J. Xi, "Design and analysis of reconfigurable parallel robots with enhanced stiffness," *Mechanism and Machine Theory*, vol. 77, 2014, pp. 92–110.

[12] Y. Jin, B. Lian, M. Price, T. Sun, and Y. Song, "QrPara: a new reconfigurable parallel manipulator with 5-axis capability," *Mechanisms and Machine Science: Advances in Reconfigurable Mechanisms and Robots II,* vol. 36, 2015, pp. 247–258.

[13] K. Miller, "Synthesis of a manipulator of the new UWA robot," in *Proc. of Austr. Conf. on Robotics and Autom.*, Brisbane, 1999, pp. 228–233.

[14] M. Maya, E. Castillo, A. Lomelí, E. González-Galván, and A. Cárdenas, "Workspace and payload-capacity of a new reconfigurable Delta parallel robot," *Int. J. Adv. Robotic Sys.*, vol. 10, no. 56, 2013, 11 pages.

[15] A. L. Balmaceda-Santamaría, E. Castillo-Castaneda, and J. Gallardo-Alvarado, "A novel reconfiguration strategy of a Delta-type parallel manipulator," *Int. J. Adv. Robotic Sys*., vol. 13, no. 15, 2016, 11 pages.

[16] M. Pfurner, "Analysis of a Delta like parallel mechanism with an overconstrained serial chain as platform," in *Proc. 14th World Congress in Mechanism and Machine Science*, Taipei, Oct. 2015.

[17] J. Brinker and B. Corves, "A survey on parallel robots with delta-like architecture," in *Proc. 14th World Congress in Mechanism and Machine Science*, Taipei, Oct. 2015.

[18] J. Brinker, N. Funk, P. Ingenlath, Y. Takeda, and B. Corves, "Comparative study of serial-parallel delta robots with full orientation capabilities," *IEEE Robotics and Automation Letters*, 2(2), 2017, additionally selected by ICRA'17 Program Committee for presentation at the conference.

[19] H. Eiselt and V. Marianov, "Foundations of location analysis," *Int. Ser. in Oper. Res. and Manage. Sci.*, vol. 155, Springer, US, 2011.

[20] C. Arbib and F. Marinelli, "An optimization model for trim loss minimization in an automotive glass plant," *Eur. J. Oper. Res.*, vol. 183, no. 3, 2007, pp. 1421–1432.

[21] K. Dowsland, E. Soubeiga, and E. Burke, "A simulated annealing based hyperheuristic for determining shipper sizes for storage and transportation," *Eur. J. Oper. Res.*, vol. 179, no. 3, 2007, pp. 759–774.

[22] J. Brinker and H. I. Gündüz, "Optimization of demand-related packaging sizes using a p-median approach," *Int. J. Adv. Manuf. Tech.*, vol. 83, 2016, 10 pages.

[23] H. Tian, M. Smith, and D. Mishra, "Optimization of packaging sizes," U.S. Patent, 8340812, Amazon Technologies, Inc., Dec. 25, 2012.

[24] Y. Won and K. Lee, "Modified p-median approach for efficient GT cell formation," *Comput. Ind. Eng.,* vol. 46, no. 3, 2004, pp. 495–510.

[25] H. Köhn, D. Steinley, and M. Brusco, "The p-median model as a tool for clustering psychological data," *Psychol. Methods*, vol. 15, no. 1, 2010, pp. 87–95.

[26] M. S. Daskin and K. L. Maass, "The p-median problem," in G. Laporte, S. Nickel, and F. Saldanha da Gama, eds., Location Science, Springer, Cham, 2015.

[27] G. L. Nemhauser, "Column generation for linear and integer programming," in M. Grötschel, ed., Optimization stories, Dt. Mathematiker-Vereinigung, Bielefeld, 2012.

[28] J. Desrosiers and M. E. Lübbecke, "A primer in column generation," in G. Desaulniers, G. Desrosiers, and M. M. Solomon, eds., Column Generation, Springer, New York, 2005.

[29] L. A. Lorena and E. L. Senne, "A column generation approach to capacitated p-median problems," in *Computers & Operations Research*, vol. 31, no. 6, 2004, pp. 863–876.

[30] J. Brinker, B. Corves, and Y. Takeda, "Kinematic performance evaluation of high-speed delta parallel robots based on motion/force transmission indices," in *Mech. Machine. T.*, 2018.

[31] J. Brinker, B. Corves, and M. Wahle, "A comparative study of inverse dynamics based on Clavel's Delta robot," in *Proc. 14th World Congress in Mechanism and Machine Science*, Taipei, Oct. 2015.

[32] T. Huang, Z. Li, M. Li, D. G. Chetwynd, and C. M. Gosselin, "Conceptual design and dimensional synthesis of a novel 2-dof translational parallel robot for pick-and-place operations," in *J. Mech. Des.*, vol. 126, no. 3, 2004, pp. 449–455.

[33] AIMMS 4.38, AIMMS B.V., software available under: http://www.aimms.com/, Haarlem, The Netherlands, 2018.

[34] S. Briot, and W. Khalil, "Dynamics of parallel robots – from rigid bodies to flexible elements," Mechanisms and Machine Science, vol. 35, Springer, 2015.

[35] T. R. Kane and D. A. Levinson, "The use of Kane's dynamical equations for robotics," *Int. J. Robot. Res.*, vol. 2, 1983, pp. 3–21.

[36] J. Angeles and S. K. Lee, "The formulation of dynamical equations of holonomic mechanical systems using a natural orthogonal complement," *ASME J. Appl. Mech.*, vol. 55, no. 1, 1988, pp. 243–244.

[37] F. M. L. Amirouche, "Computational methods in multibody dynamics," Prentice Hall, 1992.

[38] H. Josephs and R. L. Huston, "Dynamics of mechanical systems," CRC Press, 2002.

[39] Gurobi Optimization, Inc., Gurobi optimizer reference manual, software available under: http://www.gurobi.com/, 2018.